Supporting Information

Chaturvedi et al. 10.1073/pnas.1323714111

SI Methods

Genetics. Functional analyses were conducted using combination *Gal4/UAS* system (1) and *UAS-RNAi*-based genetic knockdown approach (2).

Visual Alert Response Behavior Assay. Visual alert response (VAR) assay was performed by loading overnight-starved single flies to the bottom side of a white-colored vertical chamber ($5.5 \times 2 \times 0.5$ cm). One side of the chamber was covered with a thin coverglass to allow observation. The response of the fly was captured using a digital camera connected to a computer. The chamber had a sufficient supply of air and contained one 0.4-cm-size block on the top left corner that could move back and forth across the width of the chamber. The movement of the block was manually controlled by a spring-operated mechanism. The fly was trained to acclimatize in the chamber for ∼30 min. After the training period, a drop of molasses (food) was placed on the upper side of the chamber to entice the starved flies to climb upward. As the fly reached the middle of the chamber, the block was moved from left to right across the fly visual field, and response was recorded with a video camera attached with a microscope for analysis (PixeLINK Capture OEM; Movie S1). The VAR analysis can be performed with different intensity of light as well as with different colors of blocks (a white block matched the background of the chamber and was therefore less visible, whereas a black-colored block was easily visible against the white background of the chamber). In this experiment, the data were recorded with a black-colored block.

Electroretinogram Recording. Electroretinogram (ERG) recordings were performed as previously described (3). Briefly, flies were immobilized on a box with the help of tape. To record voltage change across the eye, a recording glass microelectrode filled with Ringer's solution was gently placed on the eye surface, and a reference glass electrode filled with the same solution was placed on the thorax. Fly was allowed to adapt to the dark situation for 1–2 min and then stimulated by light pulses (4,000 lux) for ∼5 s. The signal was recorded and further amplified using a Warner IE210 Intracellular Electrometer. For each genotype, ERG was recorded for at least three times in 20 flies.

Histology and Imaging. For immunolabeling with antibodies, the brains of adult flies were dissected and fixed in fixation solution [2% (wt/vol) paraformaldehyde, 0.01 M $NaIO_4$, 75 mM lysine, 37 mM sodium phosphate buffer (pH 7.4)] for 45–60 min on ice (4). After 4 h blocking on ice with 5% (vol/vol) FBS in 0.3% Triton X-100 in PBS, brains were then incubated in preabsorbed primary antibody for overnight at 4 °C. After three washes in PBS containing 0.3% Triton X-100, brains were incubated in Alexa Fluor 488/tetramethylrhodamine isothiocyanate/Cy5-conjugated secondary antibodies (1:200) for 4 h at room temperature or overnight at 4 °C. The brains were then washed and mounted in Vectashield medium (Vector Laboratories). Images were captured using Zeiss LSM 5 Pascal laser scanning confocal microscope equipped with a Zeiss 63× Plan-Apochromat oil-immersion objective. All of the primary antibodies for histamine, carcinine, and β-alanine were first preabsorbed to reduce nonspecific staining. The following primary antibodies were used: 1:200 mouse discs-large antibody (anti-DLG) to demarcate the epithelial glia region in the lamina (4F3; Developmental Studies Hybridoma Bank), 1:200 mouse antichaoptin as photoreceptor marker (24B10; Developmental Studies Hybridoma Bank), 1:200 mouse anticysteine string protein (CSP) as synaptic vesicle marker [DCSP-1 (ab49); Developmental Studies Hybridoma Bank], 1:50 rabbit antihistamine preabsorbed with carcinine and L-histidine (Sigma), 1:50 rabbit anticarcinine preabsorbed with histamine, β-alanine, and L-histidine (ImmunoStar), 1:50 rabbit anti–β-alanine preabsorbed with carcinine (Abcam).

Quantifications of fluorescence intensities were done by selecting the area, integrated densities and mean values of three successive optic slices of an image using ImageJ software (National Institutes of Health, Bethesda).

Electron Microscopy. For normal-transmission EM, the fly heads were removed from body and fixed in 0.05 M sodium cacodylate buffer with 2.5% glutaraldehyde (pH 7.4) and processed for EM as described previously (5). After washing with cacodylate buffer, fly heads were incubated with 2% osmium tetroxide for 4–5 h at room temperature. Heads were then dehydrated in ethanol gradients (10%, 30%, 50%, 70%, 85%, 95%, 100%), incubated with propylene oxide, and embedded in PolyBed 812 resin (08792-I; Polysciences). Embedded heads were sectioned at 75 nm and then stained in uranyl acetate and lead citrate. Stained sections were mounted on copper grid and viewed at 80 kV using a Philips Tecnai 12 electron microscope.

For immunogold labeling in EM, the fly heads were fixed and embedded in LR White (London Resin Company) as described previously (6). The 100-nm sections of heads were cut and immunostained with rabbit anticarcinine antibody (1:20) followed by washing and staining with anti-rabbit secondary antibody conjugated with 15-nm gold particles. The sections were then washed in PBS and stained with 1% aqueous uranyl acetate and mounted on gold grids. The sections were examined at 80 kV using a Philips Tecnai 12 electron microscope.

The numbers of synaptic vesicles per R1–R6 photoreceptor terminals were calculated from cross-section images of the lamina by previously described single-section EM quantification methods (7). For this quantification, 10 cartridges in each of six flies ($n = 6$) were sampled, and mean for total count (N) along with their densities ($N/\mu m^2$) in photoreceptor terminals in cross-sections were calculated using Abercrombie's correction, $Nc = N\,t/(t + d)$. Where Nc is corrected vesicle number, N is raw synaptic vesicle count, t is section thickness (75 nm), and d is mean vesicle diameter (30 nm) (8).

Statistical Analysis. All of the values for quantification results are expressed as mean ± SD. The statistical significance between differences in immunostaining intensities was assessed using the two-tailed Student t test.

1. Brand AH, Perrimon N (1993) Targeted gene expression as a means of altering cell fates and generating dominant phenotypes. *Development* 118(2):401–415.
2. Dietzl G, et al. (2007) A genome-wide transgenic RNAi library for conditional gene inactivation in *Drosophila*. *Nature* 448(7150):151–156.
3. Li HS, Montell C (2000) TRP and the PDZ protein, INAD, form the core complex required for retention of the signalplex in *Drosophila* photoreceptor cells. *J Cell Biol* 150(6): 1411–1422.
4. McLean IW, Nakane PK (1974) Periodate-lysine-paraformaldehyde fixative. A new fixation for immunoelectron microscopy. *J Histochem Cytochem* 22(12):1077–1083.
5. Meinertzhagen IA, O'Neil SD (1991) Synaptic organization of columnar elements in the lamina of the wild type in *Drosophila melanogaster*. *J Comp Neurol* 305(2):232–263.
6. Han J, Reddig K, Li H-S (2007) Prolonged G(q) activity triggers fly rhodopsin endocytosis and degradation, and reduces photoreceptor sensitivity. *EMBO J* 26(24):4966–4973.
7. Meinertzhagen IA (1996) Ultrastructure and quantification of synapses in the insect nervous system. *J Neurosci Methods* 69(1):59–73.
8. Borycz JA, Borycz J, Kubów A, Kostyleva R, Meinertzhagen IA (2005) Histamine compartments of the *Drosophila* brain with an estimate of the quantum content at the photoreceptor synapse. *J Neurophysiol* 93(3):1611–1619.

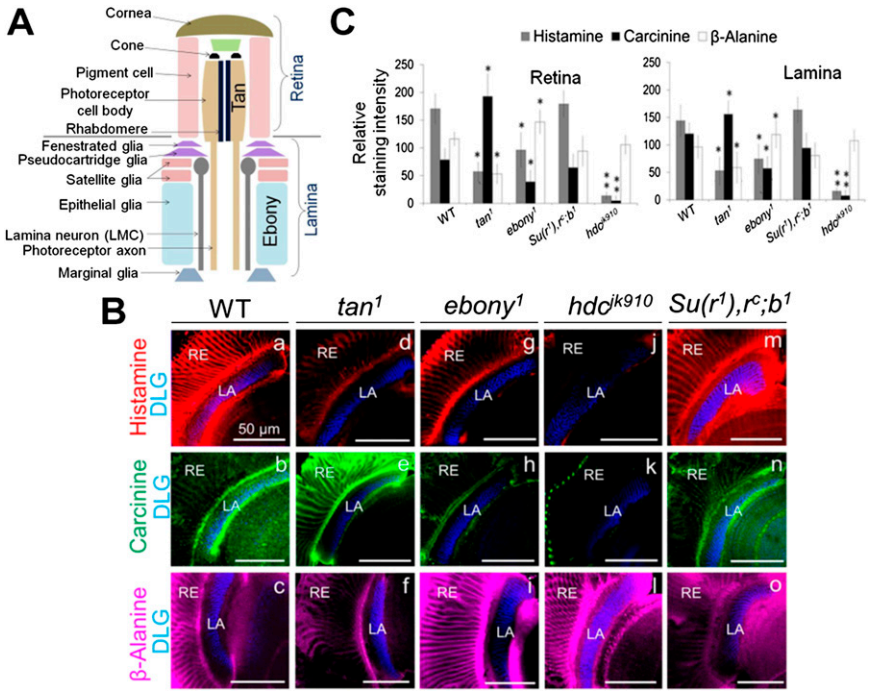

Fig. S1. Localization of histamine, carcinine, and β-alanine in the adult retina (RE) and lamina (LA) neuropil of wild-type flies (WT) and histamine metabolism mutant flies. (*A*) Schematic arrangement of pigment glial cells as well as photoreceptor cell bodies in an ommatidium of the retina and different glia layers in the lamina. (*B*) Immunolabeling of three histamine metabolism molecules: histamine (red), carcinine (green), and β-alanine (magenta) in the eyes of WT flies and histamine metabolism mutant flies. Colabeling with DLG demarcates lamina neuropil region. (*a*–*c*) Distribution of three molecules in WT flies. (*d*–*f*) tan^1 mutant flies show a reduction of histamine as well as β-alanine and an accumulation of carcinine (green) in the retina compared with WT. (*g*–*i*) $ebony^1$ mutant flies show a reduction of histamine as well as carcinine and an increase in β-alanine levels in the retina compared with WT. (*j*–*l*) hdc^{jk910} mutant flies show a dramatic reduction of histamine as well as carcinine with a slight increase of β-alanine in the retina compared with WT. (*m*–o) $Su(r^1),r^c;b^1$ mutant flies show comparable levels of histamine, carcinine, and β-alanine with WT. (*C*) Quantification of the relative immunofluorescence intensities for histamine, carcinine, and β-alanine in the lamina and the retina of WT and histamine metabolism mutant flies (*$P < 0.05$ or **$P < 0.005$, compared with WT, two-tailed *t* test, $n = 6$, for each quantification).

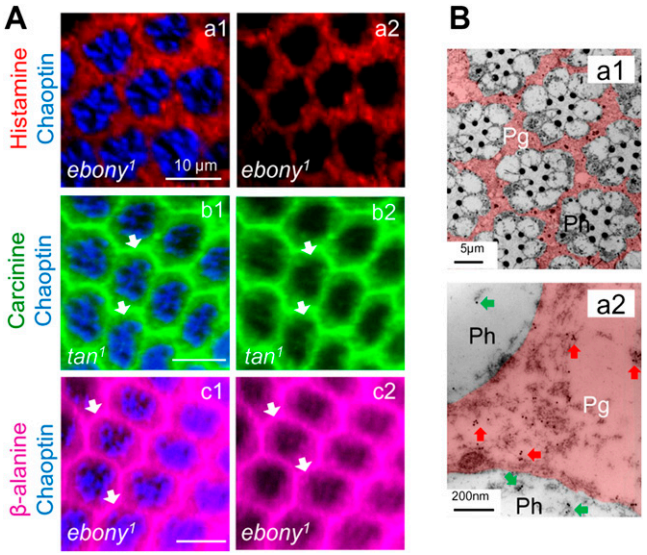

Fig. S2. Colabeling of histamine (red), carcinine (green), and β-alanine (magenta) with chaoptin (blue) in the retina of histamine recycling mutant flies, related to Fig. 1 *A* and *B*, and EM images for cone cells and ommatidium of cn^1,bw^1 fly, related to Fig. 1*C*. (*A*) Histamine metabolites in $ebony^1$ *and* tan^1 mutants. In $ebony^1$ mutant (*a1* and *a2*), histamine level is reduced in comparison with wild type (Fig. 1 *A* and *B*). In tan^1 mutant (*b1* and *b2*), carcinine level significantly increases (white arrow) in the pigment cells compared with WT (Fig. 1 *A* and *B*). In $ebony^1$ mutant (*c1* and *c2*), β-alanine level significantly increases (white arrow) in the pigment cells compared with wild type (Fig. 1 *A* and *B*). (*B*) EM images of ommatidium (*a1* and *a2*) in the retina of cn^1,bw^1 fly. Pigment cells (Pg, pink) surrounding photoreceptor cell bodies (Ph, gray). Red arrows show presence of gold particles in pigment cells, and green arrows show presence of gold particles in photoreceptor cell bodies (Fig. 1*C*).

Crosses	F1 Genotype	Genotype %
♂ *act5c-Gal4/Cyo* X ♀ *UAS-Inx2$^{RNAi:JF02446}$*	*Cyo/+;UAS-Inx2$^{RNAi:JF02446}$/+*	100
	act5c-Gal4/+;UAS-Inx2$^{RNAi:JF02446}$/+	0
♂ *act5c-Gal4/Cyo* X ♀ *UAS-Inx2$^{RNAi:KK111067}$*	*UAS-Inx2$^{RNAi:KK111067}$/Cyo*	100
	UAS-Inx2$^{RNAi:KK111067}$/act5c-Gal4	0
♂ *repo-Gal4/TM3,Sb^{1}* X ♀ *UAS-Inx2$^{RNAi:JF02446}$*	*UAS-Inx2$^{RNAi:JF02446}$/TM3,Sb^{1}*	100
	UAS-Inx2$^{RNAi:JF02446}$/repo-Gal4	0
♂ *repo-Gal4/TM3,Sb^{1}* X ♀ *UAS-Inx2$^{RNAi:KK111067}$*	*UAS-Inx2$^{RNAi:KK111067}$/+;TM3,Sb^{1}/+*	100
	UAS-Inx2$^{RNAi:KK111067}$/+;repo-Gal4/+	0
♂ *UAS-Inx2$^{RNAi:JF02446}$* X ♀ *elav-Gal4;Pin/Cyo*	*elav-Gal4/+ or y;Pin/+;UAS-Inx2$^{RNAi:JF02446}$/+*	51.7
	elav-Gal4/+ or y;Cyo/+;UAS-Inx2$^{RNAi:JF02446}$/+	48.3
♂ *UAS-Inx2$^{RNAi:KK111067}$* X ♀ *elav-Gal4;Pin/Cyo*	*elav-Gal4/+ or y;UAS-Inx2$^{RNAi:KK111067}$/Pin*	51.3
	elav-Gal4/+ or y;UAS-Inx2$^{RNAi:KK111067}$/Cyo	48.7
♂ *FM7C/y;act5c-Gal4/Cyo* X ♀ *UAS-Inx2,Inx2^{G0036}/FM7C*	*UAS-Inx2,Inx2^{G0036}/y;act5c-Gal4/+*	8.72
	UAS-Inx2,Inx2^{G0036}/y;Cyo/+	0
	FM7C/y;act5c-Gal4/+	24.54
	FM7C/y;Cyo/+	25.56
	UAS-Inx2,Inx2^{G0036}/FM7C;act5c-Gal4/+	17.04
	UAS-Inx2,Inx2^{G0036}/FM7C;Cyo/+	24.14
	FM7C/FM7C;act5c-Gal4/+	0
	FM7C/FM7C;Cyo/+	0
♂ *FM7C/y;;repo-Gal4 /TM3,Sb^{1}* X ♀ *UAS-Inx2,Inx2^{G0036}/FM7C*	*UAS-Inx2,Inx2^{G0036}/y;;repo-Gal4/+*	5.83
	UAS-Inx2,Inx2^{G0036}/y;;TM3,Sb^{1}/+	0
	FM7C/y;;repo-Gal4/+	25.04
	FM7C/y;;TM3,Sb^{1}/+	26.07
	UAS-Inx2;Inx2^{G0036}/FM7C;;repo-Gal4/+	19.04
	UAS-Inx2,Inx2^{G0036}/FM7C;;TM3,Sb^{1}/+	24.02
	FM7C/FM7C;;repo-Gal4/+	0
	FM7C/FM7C;;TM3,Sb^{1}/+	0

Fig. S3. Quantification of F1 progeny genotype obtained from Inx2 knockdown and mutant-rescued crosses, related to Fig. 2*A* table.

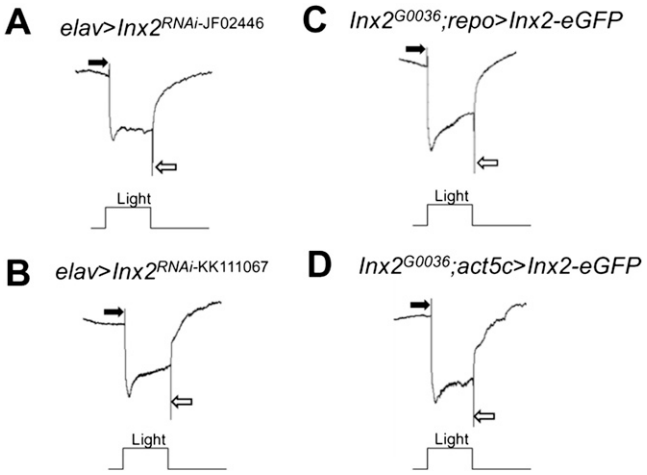

Fig. S4. Inx2 knockdown in neurons and flies rescued with Inx2 overexpression in glia show normal synaptic transmission, related to Fig. 2*A* table. Electroretinogram (ERG) of *elav*-Gal4>UAS-*Inx2^{RNAi}*-JF02446 (*A*), *elav*-Gal4>UAS-*Inx2^{RNAi}*-KK111067 (*B*), *Inx2^{G0036};repo*-Gal4>*UAS-Inx2-eGFP* (*C*), and *Inx2^{G0036}; act5c*-Gal4>*UAS-Inx2-eGFP* (*D*) flies. Black arrows indicate ON transients, and black outlined white arrows indicate OFF transients.

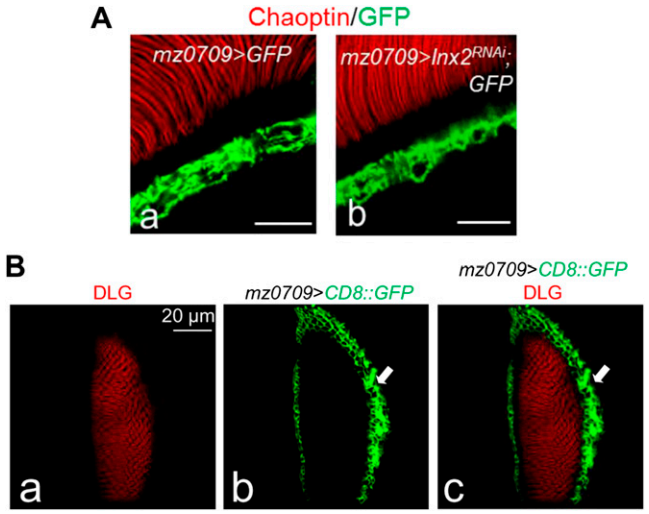

Fig. S5. mz0709-Gal4 drives expression in satellite glia of *Drosophila* lamina, related to Fig. 3. (*A*) Satellite glia labeled with *mz0709-Gal4*-driven GFP expression in the lamina of WT (*a*) and Inx2 knockdown flies (*b*). (*B*) GFP expression (green) under *mz0709-Gal4* in satellite glia of the lamina that surrounds the neuropil region immunolocalized by DLG (red) in a distal cross-section view of the lamina.

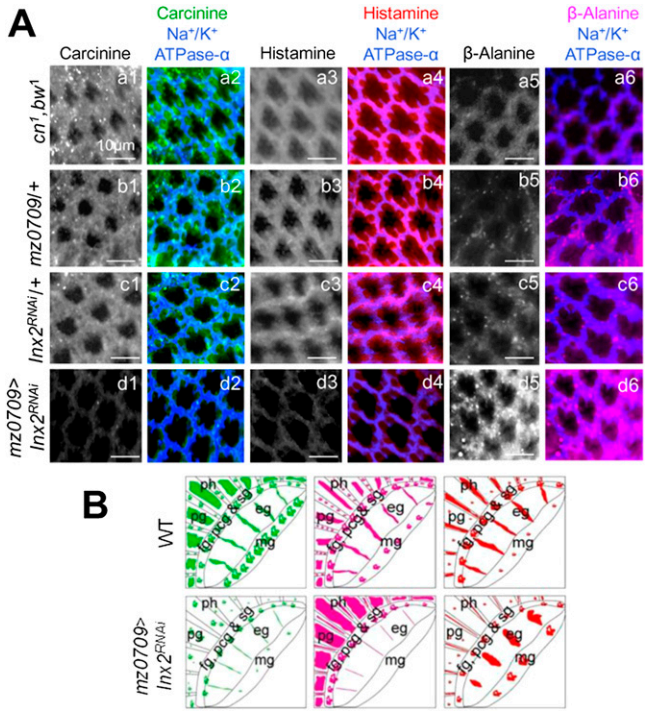

Fig. S6. Comparison of retinal histamine, carcinine, and β-alanine levels between Inx2 knockdown fly and control flies, related to Fig. 3. (*A*) Colabeling of histamine (red), carcinine (green), and β-alanine (magenta) with Na^+/K^+ ATPase-α (blue) in the retina of cn^1,bw^1 (*a1–a6*), *mz0709-Gal4/+* (*b1–b6*), *UAS-Inx2*^{RNAi}*/+* (*c1–c6*), and *mz0709-Gal4>UAS-Inx2*^{RNAi} flies (*d1–d6*). Greyscale images show single-channel signals of respective molecules. (*B*) Schematic representations of carcinine (green), histamine (red), and β-alanine (magenta) distribution in the retina and lamina of WT and *mz0709-Gal4>UAS-Inx2*^{RNAi} flies. eg, epithelial glia; fg, pcg, and sg, fenestrated glia, pseudocartridge, and satellite glia; mg, marginal glia; pg, pigment cell; and ph, photoreceptor.

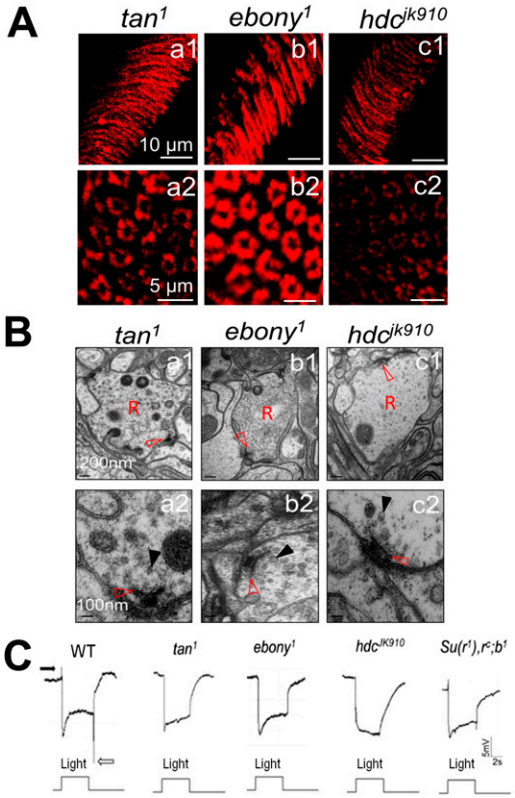

Fig. S7. Synaptic vesicles reduction in photoreceptors and visual synaptic transmission defects of histamine recycling-defective flies, related to Fig. 4. (*A*) CSP immunolabeling (red) in the lamina of *tan*^{1}, *ebony*^{1}, and *hdc*^{jk910} mutants. (*a1–c1*) Lateral views; (*a2–c2*) cross-section views. (*B*) EM images of photoreceptor terminals (*a1–c1*) in the lamina of *tan*^{1}, *ebony*^{1}, and *hdc*^{jk910} mutants. The red arrowheads point to T-bars (synapse). Magnified views of T-bars (red arrowheads) in the lamina (*a2–c2*). The black arrowheads point to synaptic vesicles in photoreceptors. (*C*) ERG traces of WT and histamine metabolism mutants [*tan*^{1}, *ebony*^{1}, *hdc*^{jk910}, and *Su(r*^{1}*),r*^{c}*;b*^{1}]. ON (black arrow) and OFF transients (white arrow) in ERG indicate synaptic transmission in WT. Absence of ON and OFF transients in ERG indicates a defect in synaptic transmission from photoreceptor to lamina neurons.

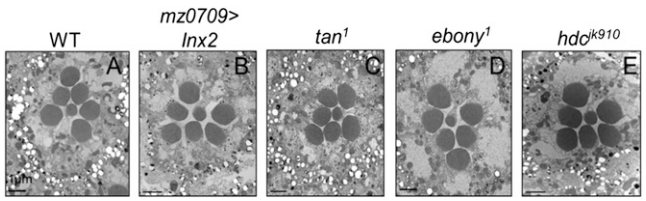

Fig. S8. Morphology of ommatidium in the retina of Inx2 knockdown flies and histamine-recycling mutants are normal, related to Figs. 3 and 4. Cross-section EM images of the retina. (*A*) WT; (*B*) *mz0709*-Gal4>*Inx2*^{RNAi} knockdown flies; (*C*) *tan*^{1}*;* (*D*) *ebony*^{1}; and (*E*) *hdc*^{jk910} flies.

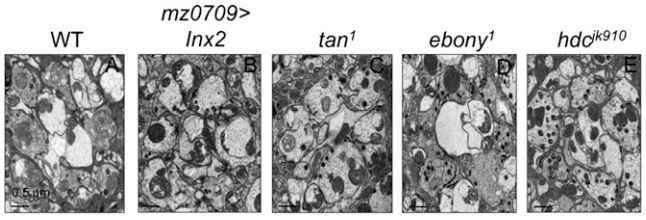

Fig. S9. Morphology of signaling units of the lamina i.e., cartridges in Inx2 knockdown flies and histamine recycling mutants are normal, related to Fig. 3 and 4. Cross-section EM images of the lamina. (*A*) WT; (*B*) *mz0709*-Gal4>*Inx2*^{RNAi} knockdown flies; (*C*) *tan*^{1}; (*D*) *ebony*^{1}; and (*E*) *hdc*^{jk910} flies.

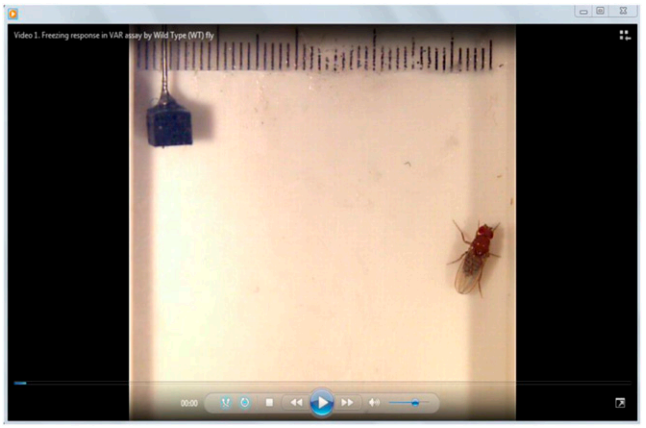

Movie S1. Freezing response in VAR assay by WT fly, related to Fig. 5.

Movie S1

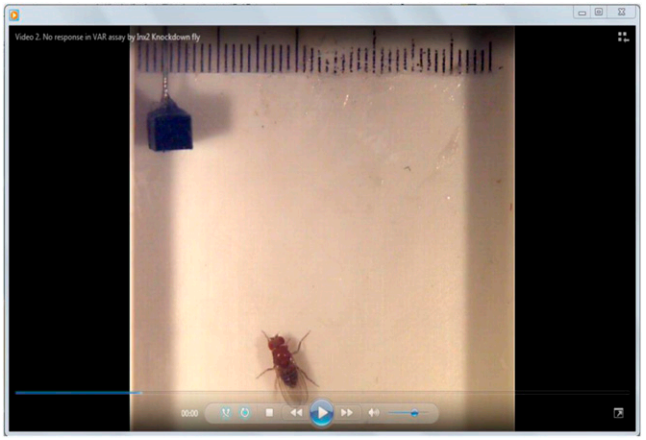

Movie S2. No response in VAR assay by Inx2 knockdown fly, related to Fig. 5.

Movie S2